Soulsby, C, Bradford, J, Dick, JJ, McNamara, JP, Geris, J, Lessels, J, Blumstock, M and Tetzlaff, D

Using geophysical surveys to test tracer-based storage estimates in headwater catchments

Article

Citation (please note it is advisable to refer to the publisher's version if you intend to cite from this work)

Soulsby, C, Bradford, J, Dick, JJ, McNamara, JP, Geris, J, Lessels, J, Blumstock, M and Tetzlaff, D (2016) Using geophysical surveys to test tracer-based storage estimates in headwater catchments. Hydrological Processes. 30 (23). pp. 4434-4445. ISSN 0885-6087

Using geophysical surveys to test tracer-based storage estimates in headwater catchments

Journal:	*Hydrological Processes*
Manuscript ID	HYP-15-0906.R1
Wiley - Manuscript type:	Scientific Briefing
Date Submitted by the Author:	14-Apr-2016
Complete List of Authors:	Soulsby, Chris; University of Aberdeen, School of Geosciences Bradford, John ; Boise State University, Geosciences Dick, Jonathan; University of Aberdeen, School of Geosciences McNamara, James; Boise State University, Geosciences Geris, Josie; Northern Rivers Institute, School of Geosciences, University of Aberdeen Lessels, Jason; University of Aberdeen, School of Geosciences Blumstock, Maria; Northern Rivers Institute, School of Geosciences Tetzlaff, Doerthe; University of Aberdeen, Northern Rivers Institute, School of Geosciences
Keywords:	Storage, Hydrogeophysics, groundwater, Tracers, Glacial drift, Electrical resistivity tomography

Using geophysical surveys to test tracer-based storage estimates in headwater catchments.

C Soulsby[1], J. Bradford[2], J Dick[1], J P McNamara[2], J Geris[1], J Lessels[1], M. Blumstock[1], and D Tetzlaff[1]

[1]School of Geosciences, University of Aberdeen, Aberdeen, UK

[2]Department of Geological Sciences, Boise State University, Boise, Idaho, USA

Abstract

Hydrogeophysical surveys were carried out in a 3.2km^2 Scottish catchment where previous isotope studies inferred significant groundwater storage that makes important contributions to streamflow. We used electrical resistivity tomography (ERT) to characterise the architecture of glacial drifts and make an approximation of catchment-scale storage. Four ERT lines (360-535m in length) revealed extensive 5-10m deep drift cover on steeper slopes, which extends up to 20-40m in valley bottom areas. Assuming low clay fractions, we interpret variable resistivity as correlating with variations in porosity and water content. Using Archie's Law as a first approximation, we compute likely bounds for storage along the ERT transects. Areas of highest groundwater storage occur in valley bottom peat soils (up to 4m deep) and underlying drift where up to 10,000mm of precipitation equivalent may be stored. This is consistent with groundwater levels which indicate saturation to within 0.2m of the surface. However, significant slow groundwater flow paths occur in the shallower drifts on steeper hillslopes, where point storage varies between ~1,000mm–5,000mm. These fluxes maintain saturated conditions in the valley bottom and are recharged from drift-free areas on the catchment interfluves. The surveys indicate that catchment scale storage is >2,000mm which is consistent with tracer-based estimates.

Key words: Storage, groundwater, glacial drift deposits, tracers

1. Introduction

Over the past two decades there has been increased awareness of the importance of groundwater in headwater environments and its contribution to stream flow (Neal et al., 1997; Soulsby et al., 1998; Haria and Shand, 2002; Uhlenbrook et al., 2004; Katsuyama et al., 2008). Despite the critical nature of this resource in maintaining downstream water supplies and ecosystem services, it is still poorly characterised (Winter et al., 2007). Advancing catchment hydrology research has been inhibited by poor integration of surface water hydrology and groundwater hydrology (Younger, 2009). Fortunately, this situation is rapidly improving and cross fertilization of methods is facilitating new insights (Miller et al., 2008; Gabrielli et al., 2010). A recent motivating theme has been to more quantitatively understand catchment-scale water storage and its relationship with stream discharge (McNamara et al., 2010; Birkel et al., 2011). There has also been increased awareness of inter-linkages between dynamic storage changes, which result from changing water balance components, and total storage, which governs solute mixing and transport (Soulsby et al., 2011; Birkel et al., 2014). Indeed, reconciling the difference between the timing of the celerity of hydrological response and the travel time of water molecules in different water stores has been identified as a key challenge in developing appropriate modelling strategies for groundwater – surface water interactions (Kirchner, 2004, McDonnell and Beven, 2014).

Despite this, groundwater storage remains poorly understood in most upland experimental catchments. Installation of boreholes is usually spatially limited due to costs and logistics, so extrapolation is difficult (Haria and Shand, 2002). Techniques which provide spatially integrated insights include the examination of spatial and temporal patterns of tracers in stream water and springs. Variations in natural isotopes or geochemicals can be used to identify the provenance and age of water sources and dynamics of their fluxes (e.g. Haria et al., 2012). Such approaches have been used in the Bruntland Burn; a sub-basin of the Girnock experimental catchment in the Scottish

Highlands (Blumstock et al., 2015). In particular, estimates of storage in the Bruntland catchment have been derived from the input-output dynamics of stable isotopes. These estimates have been derived from transit time analysis including using simple mean transit time (MTT) approximations to infer storage from the product of the MTT and water flux on weekly (Soulsby et al., 2009) or daily (Tetzlaff et al., 2014) and yielded values of ~1300 and ~1700mm, respectively. Alternatively, the use of a single passive storage term in coupled flow-tracer hydrological models (Birkel et al., 2011b) inferred up to 900mm of storage. Most recently the integration of dynamic and passive storage in a more distributed conceptual model (Soulsby et al., 2015) indicated overall variation between 2060 and 2400mm, depending upon catchment wetness. The dynamic storage is that explained by water balance changes and is typically <100mm, the passive storage is the additional storage that needs to be inferred to explain tracer damping and is an order of magnitude larger. These contrasting estimates give storages of values equivalent to 1 – 2.5 times annual precipitation, which begs the question where this storage is located in a catchment with thin soils and solid geology of low permeability (Tetzlaff et al., 2014). It has been hypothesised that glacial drift deposits form the most likely source of groundwater contributing to stream flow (Soulsby et al., 2007), but this is very difficult to verify in the absence of more detailed information on catchment groundwater storage.

The last decade has seen increased application of near-surface geophysical techniques in catchment studies (Parsekian et al., 2015). Electrical resistivity tomography (ERT), ground-penetrating radar (GPR), and shallow seismic surveys have all been applied. This has helped to establish critical boundaries (e.g. soil and bedrock depths) and to provide insight into the architecture of the sub-surface as well as implications for water storage has been a significant advance (Ferre et al., 2009; Binley et al., 2015). Such geophysical methods can provide the basis for quantitative analysis of aquifer properties if these methods can be calibrated against field observations. In montane areas, geophysical surveys are labour intensive and, where available, often spatially limited to single transects. Consequently, at most upland experimental sites we know little about aquifer structure and connectivity of groundwater flow paths and how these relate to storage dynamics and stream flow generation. In glaciated areas the situation is particularly challenging due to the legacy of substantial accumulations of drift deposits that are often highly heterogeneous but may also act as significant groundwater stores. In many regions these may be more important sources of groundwater than bedrock groundwater (Soulsby et al. 1998). Hydrogeophysical techniques have outstanding potential in such environments to improve our understanding.

Here, we utilize ERT to investigate groundwater storage in an intensively monitored catchment in the Scottish Highlands. Basic hydrometric data have been collected since 2008, soil moisture and groundwater levels have been monitored since 2011 and the stable isotope composition of precipitation and stream water have been determined since 2008 on a weekly or daily basis. Empirical and modelling studies have used hydrometric and tracer data to infer significant (>1000mm) groundwater stores in drift (e.g. Soulsby et al., 2007; Birkel et al., 2010; Tetzlaff et al., 2014). However, the distribution, thickness and properties of these drifts were unknown. Our objective here is to use spatially distributed ERT surveys to characterise these features and extrapolate the results to the catchment scale using geostatistical techniques to make a tentative approximation of catchment-scale water storage that can be compared with estimates derived from those independently derived from the input – output dynamics of stable isotopes.

2. **Study site**

The Bruntland Burn (BB) is a tributary of the Girnock experimental catchment in the Cairngorm Mountains of Scotland (Fig. 1a). The site is a headwater of the River Dee, one of the UK's most important rivers which sustains an economically important Atlantic salmon fishery, has EU conservation designations and provides drinking water for 250,000 people living in the city of Aberdeen. The BB elevation ranges between 220 and 560m and strongly reflects a glacial legacy with a valley that has been over widened and over deepened by glacial erosion (Fig, 1b). The geology is mainly granite and associated metamorphic rocks; these have poor aquifer properties and limited groundwater storage (Fig. 1c). Around 60% of the catchment is covered by various glacial drift deposits (Soulsby et al., 2007). The steeper hillslopes are mantled by lateral moraines and ice marginal deposits. These are generally freely draining and shallow podzolic soils (<0.7m deep) (Fig 1d). In the flat, wide valley bottom, extensive peat deposits have formed, with peat or peaty gley soils covering about 30% of the catchment (Tetzlaff et al., 2007). Some slightly (<10m) elevated areas in the valley bottom reflect hummocky moraines. The peats range between 0.5 to 4m deep. Beneath the peat is a shallow (0.2m) silty weathered layer which overlies thicker, coarser minerogenic drifts. The drifts are exposed locally in quarries and reveal undifferentiated material which has a high content of boulder-cobble sized clasts within a sandy-silt matrix. Given the granitic bedrock, cold temperatures and relatively young age of the soils, the clay content of the drift is low. Above 400m, thin regosols dominate, usually overlying the bedrock.

Precipitation averages ~1000mm per year and is generally evenly distributed, both seasonally and spatially. Shallow groundwater wells (1-2m deep and screened in the lower 0.2m) reveal that the water table is within 0.2m of the soil surface in the peats and peaty gley soils (Table 1). In contrast, on the steeper hillslopes the water table varies between about 1.5m deep in prolonged dry periods and 0.2m in the wetter periods (Tetzlaff et al. 2014). Water tables are very transient in the shallow regosols and underlying bedrock which have limited storage. Fuller details of the groundwater dynamics are given by Blumstock et al., (2016). Stream flow generation in the catchment has been extensively investigated (Tetzlaff et al., 2007, 2014; Birkel et al., 2011, 2014; Soulsby et al., 2015). The stream has a flashy hydrological regime, with surface runoff generation from the saturated peat soils dominating the storm period response (Figure 2). However, baseflows are also persistent and geochemically based hydrograph separation has indicated that around 30% of annual stream flow comes from deeper groundwater assumed to be in the drift (Birkel et al., 2011).

Previous isotope studies have revealed very marked damping of precipitation signals in the stream isotope response, though seasonal shifts between more and less depleted runoff in winter and summer, respectively, reflect precipitation inputs with the greater winter recharge reflected in more negative isotopes in stream flow (Figure 2). Precipitation was sampled at the weather station and stream water at the autosampler at the catchment outfall (Fig. 1). As noted in the introduction, various analyses of these isotope data imply large volumes of water storage (ca. 900-2500mm) need to be invoked to explain the mixing and damping of precipitation inputs (Birkel et al., 2011b, 2014). In part, this storage (ca. 300mm) can be explained by mixing in soil waters as much of the damping occurs in the upper soil profiles (Table 2). However, additional mixing in groundwater and the poor aquifer properties of the solid geology points to the likely importance of the drift as the major active groundwater store.

3. Methods

3.1 Transect locations

We strategically sited four transects for the ERT survey, positioned to gain coverage of the main heterogeneities in the valley bottom and build on existing hydrological infrastructure. Transect 1 (T1 – 460m) was approximately aligned north-south along an intensively monitored hillslope that covers the main landscape units and has been described by Tetzlaff et al. (2014). Transect 2 (T2 – 540m) was slightly west of Transect 1 along a line that was characterised by a lower coverage of saturated soils as it mainly crossed hummocky moraines. Transect 3 (T3 = 360m) was aligned roughly south west – north east at the head of the valley, directly upslope from the confluence of 3 headwater tributaries of the BB. Transect 4 (T4 – 400m) was also aligned to a similar orientation over an area of peat bog that forms part of the most northerly headwater of the BB. The surveys were undertaken over a week-long period in August 2013; this was in the middle of a warm dry summer, so the catchment was relatively dry; and the water table was close to the minimum levels shown in Table 1.

3.2 Electrical resistivity measurements and data processing

Electrical resistivity measurements are made using four electrodes inserted into the ground. Current is driven through two of the electrodes (the source) and potential difference is measured between the other two electrodes using a resistivity meter (Ward, 1990). In ERT surveys, this measurement is repeated many times with differing separation between the electrodes. When the electrodes are further apart, a higher proportion of the current flows deeper in the earth and consequently, the measurement is sensitive to deeper structures. In ERT imaging, we use tomographic inversion techniques, similar to those used in medical imaging, to estimate the earth structure beneath the survey. The input data are either the resistance (ratio of potential to current) or apparent resistivity which is the equivalent homogeneous earth model which would produce the potential observed for a particular electrode combination. The output of the inversion is an estimate of the earth's resistivity structure as a function of space.

We acquired electrical resistivity measurements along each transect using an IRIS Instruments SysCal Pro, 72 electrode system with 5 m electrode spacing and rolled the electrode array in overlapping segments to compile the long profiles. We collected data in both dipole-dipole and Wenner electrode geometries (Zonge et al., 2005), then combined measurements into a single inversion. For the dipole-dipole measurements, we acquired six depth levels with a minimum dipole-dipole centre distance of 10 m and a maximum of 35 m. In the Wenner arrays, we utilized 16 depth levels with a minimum *a* spacing (potential electrode spacing) of 5 m and a maximum of 80 m. We were able to use more than 96% of the data. We rejected data if the deviation exceeded 3%, if there was a negative resisitivity, or if the injection current was less than 0.5 mA. These were the primary sources of error and were identified as default parameters in the IRIS syscal autofiltering routine.

We inverted the electrical resistivity data using the commercial software package Res2Dinv. Topography (from LiDAR) was incorporated using a distorted finite-element grid, and the inversion was calculated using the standard least-squares constraints. We took the depth to the bedrock interface to be the 2000 Ω m contour in the ERT result. While this resistivity is substantially lower than the resistivity of unweathered granite, it is substantially higher than the resistivity of water saturated unconsolidated sediments and formed the mid-point of transition between the two to an error of around $\pm$10%. With regularization during the inversion, the ERT image was smoothed laterally and vertically and obtaining a precise estimate of depth-to-bedrock was not possible. However, the 2000Ωm contour was roughly centered on the vertically smeared sediment/bedrock transition and provides a reasonable estimate of depth-to-bedrock.

3.3 *Storage estimates*

To estimate liquid water content, we utilized Archie's Law and assumed that the clay content was negligible. This is a reasonable assumption based on prior soil characterization at the site and the size distribution of the sediments (Moir et al., 2002; Geris et al., 2015). Further, we assumed that the profiles were fully water saturated. With these assumptions, we rearrange Archie's Law to give the following equation for volumetric water fraction (θ_w):

$$\theta_w = \left(\frac{\rho_w}{\rho}\right)^{\frac{1}{m}} \tag{1}$$

where ρ_w is the resistivity of the pore water, ρ is the bulk measured resistivity, and m is the Archie's Law exponent known as the cementation factor (Knight et al., 2005). Both ρ_w and m are unknowns.

We estimated the likely range of values for ρ_w from surface water measurements. During low flow conditions, the stream is primarily derived from deeper groundwater in the drift (Birkel et al., 2015). Typical surface water conductivity (σ_w) during these low flow conditions is 125 µS cm^{-1} which was used as a first approximation of groundwater conductivity. We take the inverse of this to approximate ρ_w= 80 Ω·m in Eqn 1. Previous studies suggest that in unconsolidated sediments, a reasonable range for the cementation factor, m, is 1.3 – 2.0 (Knight, 2005). To estimate uncertainty in water content, we used the lowest cementation factor value to calculate the minimum likely θ_w, and the highest value to calculate the maximum likely θ_w. We used the central value of m=1.65 to determine our best estimate of θ_w.

To calculate soil and groundwater storage, we vertically integrated the estimated θ_w from the approximate bedrock interface to the surface along the transect. We repeated this calculation three times with the minimum, best estimate, and maximum values of θ_w. There are four important caveats to our approach. First, we are assuming full water saturation from bedrock to surface. This assumption is not strictly correct, however, depth to the water table is shallow, variable and unknown along each transect (e.g. Table 1). Assuming full saturation results in a small overestimate of water content, but since the vadose zone is very thin (generally <1-2 m) this error will not contribute significant error. The second caveat is the use of Archie's Law to calculate water content in the peat which is up to 4 m thick along T1 and T4. Comas and Slater (2004) found that organic soils do not strictly follow the Archie's Law dependency. Additionally, the conductivity of water in peaty soils tends to be lower than that in the deeper groundwater. However, our approach found water content in the peat >0.6 which compares well with measured values (Geris et al., 2015). Given that the peats only comprise 10-15% of the sediment column in the base of the valley where they are found, these uncertainties probably have a small effect on any errors in the bulk storage calculation. Thirdly, we assumed that there is no clay in the system. If there were clay, the decreased bulk resistivity in the system due to conduction along the grain surfaces would result in an overestimate of volumetric water content using (1). However, the generally high measured resistivities, and coincidence of low resitivties with areas of peat also suggest that clay content is low corroborating the field evidence cited above. Finally, Archie's Law has not been calibrated to boulder-rich deposits. Although in the catchment some boulder moraine deposits are present mainly as lateral moraines, these appear to be mainly surficial. Exposures of deeper deposits in sand quarries indicates that the drift is mostly coarse sand-silty material with some pebble-cobble sized clasts. Thus the boulders are a likely small percentage of the drift composition and the errors will be relatively low.

From the point storage estimates along each transect, we extrapolated a first approximation of catchment-scale storage using a regression-kriging based approach (Odeh et al., 1995). It was recognised with only four transects that this approach would not fully capture the heterogeneity at the catchment scale, but could provide a useful first step. This method requires the use of a predictive model to estimate storage and the combination with the kriged residuals of these estimates. In this study we have applied the Cubist model which is a form of a rule based regression as outlined by (Quinlan, 1992) to estimate the storage. The storage estimates derived from the ERT surveys were averaged to create a ten metre grid along each transect. To fit the Cubist model many covariates were considered, but due to the limited spatial coverage of the transects, only the digital elevation model and the height from the stream was included. As the observations were focused in the lower part of the catchment, the model was only used to estimate storage in this area, according to Rodriguez and Enghofer (2004) using the SAGA GIS software (Böhner and Selige, 2006). The Cubist model was trained using 75% of the transect observations using 10 fold cross validation using the caret package (Kuhn, 2008) within the R programming environment (R Core Team, 2012). The residuals of the Cubist model within the training set with the lowest RMSE were used to fit an exponential variogram. The regression-kriged storage estimates were evaluated using the remaining 25% of the points and showed a strong correlation (r^2 = 0.95). For extrapolation to the upper hillslpopes, the area upslope of the transects was estimated using a decaying value from the estimates available in the valley bottom to storage of 10 mm on the catchment interfluves. This is reasonable given the low storage in the exposed rocks and regosols on the interfluves (Fig 1a).

4. Results

4.1 *Resistivity and water content profiles*

The ERT surveys revealed some broad similarities between the four transects (Figure 3). All profiles had high resistivity layers near the ground surface on steeper slopes indicating areas of relatively dry, unsaturated conditions (Figure 4). In some cases, zones of high, near surface resistivity (>2000 Ω·m, θ_w<15%) corresponded to moraines with larger cobble and boulder clusters. Below the surface on the steeper hillslopes, lower resistivity (300-1500 Ω·m, θ_w=15-45%) layers were present, with some suggestion of stratification evident in an intermediate layer where drifts are likely saturated. Below these intermediate layers is a very high resistivity layer which we interpret as the unaltered bed rock, which ranges from ca. 5m deep on the upper slopes, to >40m deep in the valley bottoms. The upper few metres of the valley bottoms had low resistivities (<185 Ω·m, θ_w>60%) that correlate with the water-filled peat. Below, the valley bottoms had several tens of metres of saturated drift.

In more detail, T1 has shallow groundwater: Table 1 shows the water table variation in the upper, mid and lower hillslopes along the Transects 1 and 2, shown in Figure 1. The highest resistivities (Figure 3) indicate that the bedrock is around 1-5 m deep in the south and increases to the north, reaching a maximum of ~20m in valley bottom. The bedrock profile has stepped increases in depth and drift thickness at 50 m and 125m. The low point in the profile occurs around 380m along the transect, then the drift thickness begins to decrease. Note that the high point between 300 and 350 m is likely a resisitivity high point but the apparent bedrock peak is probably an artefact of smoothing in the inversion. In the shallow hillslope drifts, low resistivity values imply saturated low porosity material extending downslope to ~100m. Thereafter, a drier/less porous area is indicated by higher resistivities, which correspond to bouldery moraine deposits just above the break in slope in topography at 300m. These thicken downslope, notably between 160-280m with very high resistivities in the upper few metres of the subsurface. This overlies drift with higher water content and lower resistivities similar to those measured in the upper slope. The very low resistivities in the valley bottom from about 300m along the transect imply high water content (>0.6) in the upper few metres of the riparian zone (Figure 4), broadly consistent with measured (with gravimetrically calibrated TDR probes) high water content in the peat (>0.8). The sharp definition of the lower boundary of this low resistivity layer is consistent with the fine textured mineral zone immediately beneath the peat. Increased resistivities below are consistent with the lower porosity minerogenic drift.

T2 was almost parallel to T1, though sited to cross a drier part of the valley. Table 1 shows water table variations at sites on or close to the transect (see Figure 1). At a depth of ~30 m, the southern end of T2 has deeper bedrock than T1. The bedrock depth is roughly constant across the central valley, until it begins to shallow after around 350m (Fig. 3). Again, there are suggestions of steps in the bedrock depth at around 350m and 450m. At 300m the bedrock is around 30m deep, but this decreases to the north and is around 15m below the lower scree slope at the end of T2 (Fig 1). Shallow zones of low resistivity are in the upper 1-2m of the profile; these occur between 80 – 150m where wetter peaty gley soils occur (Fig. 4), then again at 230-290m where peat fringes the stream and at 360-450m where there is a patch of more peaty soils. Higher resitivities in the near surface implies drier/lower porosity material at 0-75 m and 290-360m which correspond to slightly elevated hummocky moraine material. Beyond 450m, the lower slope has higher resistivity consistent with the free-draining nature of the bouldery screes. However, below this, more moderate resistivities infer saturated deposits of lower porosity, which are fairly contiguous across the valley bottom in the lower 20m or so of the drift.

T3 is aligned west-east; in the west the bedrock is inferred at ~20m deep (Fig. 3). This increases to around 40m deep at 150m, thereafter the inferred bedrock surface has a reduced gradient with the drift remaining around 40m thick. It should be noted that 40 m depth is just at the limit of depth resolution for the ERT array we used so the uncertainty in the depth estimate is greatest here, with the potential that the rock boundary could be even deeper. However, the clear increase in resistivity indicates that bedrock cannot be much deeper than the interpreted value. Between 50-170m, the surface of the hillslope has a very high resistivity, low water content (Fig. 4) zone, around 5-10m thick, that coincides with extensive superficial drifts comprising bouldery lateral moraine deposits. A low resistivity layer is evident in the hillslope between 0 and 170m, implying a 10-20m thick zone of high water content “sandwiched” between the bedrock and boulder moraines (Fig. 4). The western end of T3 began in a wetland area, characterised by surface saturation. Wetlands are also evident between around 170 m and 190 m and after 250m with very low resistivities in the upper 2m, consistent with the peat soils and similar to the lower part of T1. However, resistivities rise at depths below 2m for much of the valley bottom, again implying lower porosity and water storage.

T4 is similar to T3. The western edge of the slope has almost continuous moraine cover up to 170m which is characterised by a high resistivity layer in the upper 5-10m. This cover is broken between around 70-90m where the surface slope flattens and a patch of low resistivity material coincides with a small wetland area. Between 80 – 170m the high resistivity moraine thickens into a distinct ridge before terminating at the edge of a flat area with very low surface resistivities where a raised bog of high water content (Fig. 4) is located in the valley bottom. After around 300m the slope increases again on the eastern side of the valley. Here, surface resistivities increase in the upper 5m corresponding to the toe of a scree slope similar to T2. The bedrock rock surface is picked out by a high resistivity transition which is around 10m deep on the western slopes. There is a sharp drop in bedrock depth at about 80 m. Beyond this, the depth to bedrock increases to about 20m followed by a second step and increase in depth to ca 40m depth at 180m along the transect. The bedrock surface again appears to flatten before the gradient steepens from 230m. At 250m the bedrock appears >40m below the surface and is below the depth sensitivity of our ERT array. At 290m there is a near-vertical increase in the bedrock surface bringing it to within 30m of ground level. The subsurface drift below the hillslope and valley bottom has a higher resistivity than the over-lying saturated peat. This moderate resistivity infers water filled sediments with moderate porosity.

4.2 *Catchment storage estimates*

For each ERT transect the depth-integrated water storage at a point along the transect was estimated (Figure 5). All four transect lines were similar in that the highest storage was generally in the central part of the valley where the drifts were thickest and decreased on the steeper slopes. Depth equivalents of point water storage ranged between <1m at the southern ends of T1, T2 and T4, to over 10m in the central parts of T3 and T4 where the depth to bedrock was greatest, and coincided with deeper valley bottom peats. The uncertainties around the estimates are unavoidably large (in the order ±30%), but the marked variations in storage distribution are very insightful. In particular, the analysis highlights the marked differences between the large volumes of storage in the lower parts of the catchment and the lower storage on the steeper, upper hillslopes.

The extrapolation of the transect storage estimates using the cubist regression and kriging described in the methods section gives a tentative first approximation of catchment-scale storage in the soils and drifts (Figure 6). This approximation re-emphasises the distribution of valley bottom storage and how storage increases to the west of the catchment. It also shows the low (<1m) storage over much of the catchment on the steeper slopes and catchment interfluves. Averaged over the catchment, total storage is estimated at 2050-2300mm with an approximate uncertainty of around ±700mm.

5. Discussion

The application of ERT in the Bruntland catchment has provided a further step towards characterising the nature and size of shallow groundwater stores at this glaciated, drift-filled site. As with other studies in similar settings, this has helped to characterise the heterogeneity in the drift (e.g. Koch et al., 2011) and the bedrock interface (e.g. Miller et al., 2008). The study has also shown the extent and depth of lower resistivity zones of high water storage in valley bottom peats, where near-surface water tables in the riparian zone govern the flashy response of the stream in runoff events (Sheib et al., 2008; Cassidy et al., 2014). In contrast, high resistivity surface layers pick out the location of sandy hummocky moraines which create elevated areas in the valley bottom (e.g. in T1 and T2), and more bouldery lateral moraines at the side of the valley in T3 and T4. Below these layers, the extent and depth of the drift fill in the valley was extensive. Whilst the lower valley slopes (up to around 400m) were covered with 1-7m thick drift, the drift was thickest with 20 to > 40m depths in the valley bottom. Differences in resistivity of the drift infer differences in the porosity and water content. However, given the high water tables, even on the steeper hillslopes, it appears that the drift is usually water filled and provides a main source of groundwater seepage to the valley bottom and stream channel (Blumstock et al., 2005). It is likely recharged by vertical drainage in the steeper slopes and through the moraines in the valley bottom (Soulsby et al., 2015). In addition, fluxes from the upper hillslopes above that are free of drift cover and where storage is limited are likely a major source of rapid recharge down slope in precipitation events. This latter mechanism probably contributed to the hillslopes low resistivity/high water content layers in the western part of T3 and T4 (Figs. 3 and 4).

One of the main motivations for characterising the drift geology and estimating the water storage was to understand better the context of mixing and tracer damping that is evident in rainfall-runoff transformations in the catchment (Figure 2). Integrating the ERT surveys with the geostatistical analysis summarised in Figure 6 provided a novel means of doing this. Previous tracer-based estimates of storage in the Bruntland catchment derived from isotope input-output dynamics have given a range of values between ~1000 and 2400mm (e.g. Soulsby et al., 2015). Clearly, these approaches have simplifying assumptions, but the similar orders of magnitude for these tracer and independent geophysics (ca 2050-2300 mm) based estimates indicate reasonable convergence. It should be noted that the surveys were undertaken in the summer of 2013 which coincided with the middle of a prolonged dry warm period. Detailed analysis of soil moisture and groundwater level data in the catchment revealed that dynamic storage changes were limited to deficits of -40mm in the peat soils and -100mm in the podzols (Geris et al., 2015). Thus, the ERT surveys and inversion would probably have revealed greater storage if undertaken in a wet period, though the summer deficits are <5% of the total storage estimates, so the effect is probably relatively minor.

Of course, it should be emphasised that the estimates presented here are restricted to the soil and drift. The sharp definition of the high resistivity of the bedrock is consistent with the poor aquifer properties of the underlying granitic and metamorphic rocks. However, the granite in particular has fractures in the upper 5-10m which may act as groundwater flow paths (e.g. Comte et al., 2012). However, their main role appears as active recharge areas where outcrops occur above the glacial trim line. The infilling of drift appears to restrict their effectiveness as conduits of deeper groundwater movement, though, of course, there may be additional storage. The role of fractures may allow granite on north and south sides of the catchment to sustain seepages and springs where groundwater re-emerges in the saturated valley bottom (Blumstock et al., 2015).

To better elucidate the storage characteristics of the drift and bedrock, drilling would be needed to calibrate the stratigraphy of the drifts more quantitatively. Installation of deep bore holes would allow testing the aquifer properties (Scheib et al., 2010). However, this is very expensive, intrusive and gives only point specific information. In the meantime, the advantage of ERT surveys is that they are relatively rapid, non-intrusive and spatially extensive. Thus, increasing the number of transects, especially in the upper parts of the catchment, could be a more efficient means of constraining the storage estimates as it would help refine the geostatistical analysis used to derive Figure 6. However, perhaps more important to improving the local detail, is to use the new geophysical methods to better upscale our understanding of such headwater catchments in terms of groundwater – surface water interactions in mesoscale basins (Binley et al., 2015).

Such improved characterisation and identification of significant groundwater stores is a prerequisite to enhancing models of catchment groundwater-surface water interactions that can test assumptions about how mixing processes damp tracer inputs in precipitations. Although the images shown in Figures 4-6 allow visualisation of the distribution of storages and likely interconnections, only a more physically-based coupled flow-tracer model will allow the fluxes associated with mixing and transport to be understood in a spatially explicit way (Ala-aho et al., 2015).

6. Conclusion

We showed ERT surveys to be highly informative in identifying areas of groundwater storage in drift-filled montane catchments. This allowed an approximation of total catchment storage estimates of around 2300mm that are consistent with estimates derived from a variety of tracer-based methods. ERT has potential as a rapid appraisal tool for qualitatively assessing ground water in montane catchments and providing guidance for targeted drilling to improve quantification of aquifer properties and invaluable information for linked flow-transport models to test hypotheses about catchment hydrological function. It is also amenable to geostatistical techniques that can help extrapolate to the catchment scale.

Acknowledgements

The authors are grateful to Stian Bradford, Chris Gabrielli, and Julie Timms for practical and logistical assistance. The provision of transport by Iain Malcolm and Ross Glover of Marine Scotland Science was greatly appreciated. We also thank the European Research Council ERC (project GA 335910 VEWA) for funding through the VeWa project and the Leverhulme Trust for funding through PLATO (RPG-2014-016).

References

Ala-aho, P., Rossi, PM., Isokangas, E., Kløve, B. & Ala-Aho, POA. (2015). 'Fully integrated surface-subsurface flow modelling of groundwater-lake interaction in an esker aquifer: Model verification with stable isotopes and airborne thermal imaging'. *Journal of Hydrology*, vol 522, pp. 391-406.

Binley, A., S. S. Hubbard, J. A. Huisman, A. Revil, D. A. Robinson, K. Singha, and L. D. Slater, 2015, The emergence of hydrogeophysics for improved understanding of subsurface processes over multiple scales, Water Resources Research, 51, doi:10.1002/2015WR017016.Binley et al., 2015).

Birkel, C., D. Tetzlaff, S. M. Dunn, and C. Soulsby (2010), Towards simple dynamic process conceptualization in rainfall-runoff models using multi-criteria calibration and tracers in temperate, upland catchments, Hydrol. Processes, 24, 260–275.

Birkel, C., Tetzlaff, D., Dunn, S. M., and Soulsby, C.: Using time domain and geographic source tracers to conceptualize streamflow generation processes in lumped rainfall-runoff models, Water Resour. Res., 47, W02515, doi:10.1029/2010WR009547, 2011a.

Birkel, C., Soulsby, C., and Tetzlaff, D.: Modelling catchment scale water storage dynamics: reconciling dynamic storage with tracer-inferred passive storage, Hydrol. Process., 25, 3924–3936, 2011b.

Birkel, C., C. Soulsby, and D. Tetzlaff (2015), Conceptual modelling to assess how the interplay of hydrological connectivity, catchment storage and tracer dynamics controls non-stationary water age estimates. Hydrol. Process., DOI: 10.1002/hyp.10414.

Blumstock, M. Tetzlaff, D. Malcolm, I.A. Nuetzmann, G. and Soulsby, C. (2015) Baseflow dynamics: multi-tracer surveys to assess groundwater contributions to montane streams under low flows. *Journal of Hydrology*. doi:10.1016/j.jhydrol.2015.05.019

Blumstock, M., Tetzlaff, D. Dick, J.J. Nuetzmann, G. and Soulsby, C. (2016) Spatial organisation of groundwater dynamics and stream flow response from different hydropedological units in a montane catchment. *Hydrological Processes.* DOI: 10.1002/hyp.10848

Böhner, J., Selige, T., 2006. Spatial prediction of soil attributes using terrain analysis and climate regionalisation. SAGA-Analysis Model. Appl. Göttingen, Göttinger Geogr. Abhandlungen 13–28.

Cassidy, R., Comte, J-C, Nitsche, J., Wilson, C., Flynn, R. & Ofterdinger, U. (2014). 'Combining multi-scale geophysical techniques for robust hydro-structural characterisation in catchments underlain by hard rock in post-glacial regions'. *Journal of Hydrology*, vol 517, pp. 715-731.

Comas, X., and L. Slater, 2004, Low-frequency electrical properties of peat: Water Resources Research, **40**,W1214. doi: doi:10.1029/2004WR003534.

Comte, J-C, Cassidy, R., Nitsche, J., Ofterdinger, U., Pilatova, K. & Flynn, R. (2012). 'The typology of Irish hard-rock aquifers based on an integrated hydrogeological and geophysical approach'. *Hydrogeology Journal*, vol 20, no. 8, pp. 1569-1588.

Daily, W., A.Ramirez, A. Binley, and D. LaBreque, 2005, Electrical Resistance Tomography—Theory and Practice, in Dwain K. Butler, ed., Near Surface Geophysics: Society of Exploration Geophysicists.

Ferré, T., L. Bentley, A. Binley, N. Linde, A. Kemna, K. Singha, K. Holliger, J. A. Huisman, and B. Minsley (2009), Critical Steps for the Continuing Advancement of Hydrogeophysics, Eos Trans. AGU, 90(23), 200–200, doi:10.1029/2009EO230004.

Gabrielli, C. P., McDonnell, J. J., & Jarvis, W. T. (2012). The role of bedrock groundwater in rainfall-runoff response at hillslope and catchment scales, *Journal of Hydrology*, 450, 117–133. doi:10.1016/j.jhydrol.2012.05.02

Geris, J., Tetzlaff, D., McDonnell, JJ and Soulsby (2015). The relative role of soil vs tree cover on water storage and transmission in Northern catchments. *Hydrological Processes.* DOI:10.1002/hyp.10289.

Geris, J. Tetzlaff, D and Soulsby C. (2015) Resistance and resilience to droughts: hydropedological controls on catchment storage and runoff response. *Hydrological Processes.* DOI: 10.1002/hyp.10480.

Haria, A. H., & Shand, P. (2004). Evidence for deep sub-surface flow routing in forested upland Wales: implications for contaminant transport and stream flow generation. *Hydrology and Earth System Sciences*, 8, 334-344. doi:10.5194/hess-8-334-2004

Haria, A., Shand, P., Soulsby, C., and Noorduijn, S. (2013) Spatial delineation of groundwater-surface water interactions through intensive in-stream profiling in the Hafren headwater catchments, Plynlimon, UK. *Hydrological Processes.* DOI:10.1002/hyp9551.

Katsuyama, M., Fukushima, K., & Tokuchi, N. (2008). Comparison of Rainfall-Runoff Characteristics in Forested Catchments Underlain by Granitic and Sedimentary Rock with Various Forest Age. *Hydrological Research Letters*, Vol. 2, pp.14-17. doi: 10.3178/HRL.2.1.

Kirchner, J.W., X. Feng, C. Neal, and A.J. Robson, The fine structure of water-quality dynamics: the (high-frequency) wave of the future, *Hydrological Processes*, 18, 1353-1359, 2004.

Koch K, Wenninger J, Uhlenbrook S, Bonell M. 2009. Joint interpretation of hydrological and geophysical data: Electrical resistivity tomography results from a process hydrological research site in the Black Forest Mountains, Germany. Hydrological Processes 23: 1501–1513. DOI: 10.1002/Hyp.7275

Kuhn, M., 2008. Building predictive models in R using the caret package. J. Stat. Softw.

McDonnell, J. J.*, and* K. Beven *(*2014*),* Debates—The future of hydrological sciences: A (common) path forward? A call to action aimed at understanding velocities, celerities, and residence time distributions of the headwater hydrograph*,* Water Resour. Res.*,* 50*,* 5342–5350*, doi:*10.1002/2013WR015141.

McNamara JP, Tetzlaff D, Bishop K, Soulsby C, Seyfried M, Peters NE, Aulenbach BT, Hooper R. 2011. Storage as a Metric of Catchment Comparison. *Hydrol. Process.* **25**. DOI: 10.1002/hyp.8113

Miller, C., Routh, P., Brosten, T. and McNamara, J.P, 2008. Application of time-lapse ERT to watershed characterization. Geophysics 73(3), G7-G17, DOI:10.1190/1.2907156.

Moir, H., Soulsby, C. and Youngson, A.F. (2002) The hydraulic and sedimentary controls on the availability of Atlantic salmon spawning habitat in the river system NE Scotland. *Geomorphology.* 45, 291-308.

Neal, C., Hill T, Hill, S., & Reynolds B. (1997). Acid neutralizing capacity measurements in surface waters and groundwaters in the upper Severn, Plynlimon: from hydrograph splitting to water flow pathways. *Hydrology and Earth System Sciences,* 3: 687–696. doi:10.5194/hess-1-687-1997

Odeh, I.O.A., McBratney, A.B., Chittleborough, D.J., 1995. Further results on prediction of soil properties from terrain attributes: heterotopic cokriging and regression-kriging. Geoderma 67, 215–226. doi:10.1016/0016-7061(95)00007-B

Parsekian, A.D., K. Singha, B. Minsley, W.S. Holbrook and L. Slater (2015) Multiscale Geophysical Imaging of the Critical Zone, Reviews of Geophysics, 53, doi:10.1002/2014RG000465.

Quinlan, J., 1992. Learning with continuous classes. 5th Aust. Jt. Conf. Artif. Intell.

R Core Team, 2012. R: A language and environment for statistical computing. R Foundation for Statistical Computing, Vienna, Austria, 2012.

Rodríguez A. and M. Egenhofer (2004) Comparing Geospatial Entity Classes: An Asymmetric and Context-Dependent Similarity Measure. *International Journal of Geographic Information Science* 18(3): 229-256, 2004

Scheib A.J., Arkley S., Auton C., Boon D., Everest J., Kuras O., Pearson S., Raines M., Williams J., 2008. Multidisciplinary characterisation and modelling of a small upland catchment in Scotland. Quaestiones Geographicae 27A/2, Adam Mickiewicz University Press, Poznań 2008, pp. 45–62, 12 Figs. 2 Tabs. ISBN 978-83-232-2110-4. ISSN 0137-477X.

Soulsby, C., Chen, M., Ferrier, R.C., Jenkins, A. and Harriman, R. (1998) Hydrogeochemistry of shallow groundwater in a Scottish catchment. *Hydrological Processes.* 12, 1111-1127.

Soulsby C, Tetzlaff D, van den Bedem N, Malcolm IA, Bacon PJ, Youngson AF. 2007. Inferring groundwater influences on surface water in montane catchments from hydrochemical surveys of springs and streamwaters. *J. Hydrol*. **333**: 199– 213.

Soulsby C, Tetzlaff D, Hrachowitz M. 2009. Tracers and transit times: windows for viewing catchment scale storage? *Hydrol. Process*. **23**: 3503–3507. DOI: 10.1002/hyp.7501

Soulsby, C., Piegat, K, Seibert, J. and Tezlaff, D. (2011) Catchment scale estimates of flow path partitioning and water storage based on transit time and runoff modelling. *Hydrological Processes.* DOI: 10.1002/hyp.8324.

Soulsby C., Birkel C., Geris J., Dick J., Tunaley, C. and Tetzlaff, D. (2015) Stream water age distributions controlled by storage dynamics and non-linear connectivity: modelling with high resolution isotope data. *Water Resources Research.* **DOI:** 10.1002/2015WR017888.

Tetzlaff D, Soulsby C, Waldron S, Malcolm IA, Bacon PJ, Dunn SM, Lilly A. 2007. Conceptualisation of runoff processes using GIS and tracers in a nested mesoscale catchment. *Hydrological Processes* **21**: 1289–1307.

Tetzlaff D, Birkel C, Dick J, Soulsby C. 2014. Storage dynamics in hydropedological units control hillslope connectivity, runoff generation and the evolution of catchment transit time distributions. *Water Resour. Res*., doi: 10.1002/2013WR014147.

Uhlenbrook S., Frey M., Leibundgut Ch., Maloszewski P., 2002: Hydrograph separations in a mesoscale mountainous basin at event and seasonal timescales. Water Resources Research, 38, 6, 10.1029/2001WR000398.

Ward, S. H., 1990, Resistivity and induced polarization methods, in Stanley H. Ward, ed., Geotechnical and environmental geophysics: Soc. Expl. Geophys. 147-189.

Winter T C., (2007). The Role of Ground Water in Generating Streamflow in Headwater Areas and in Maintaining Base Flow. *Journal of the American Water Resources Association (JAWRA),* 43(1):15-25. DOI: 10.1111/j.1752-1688.2007.00003.x

Younger, P.L. 2009 *Groundwater in the Environment.* Wiley.

Zonge, K., J. Wynn, and S. Urquhart, 2005, Resistivity, Induced Polarization and Complex Resisitivity, in Dwain K. Butler, ed., Near-Surface Geophysics: Society of Exploration Geophysicists. 265-300.

List of Tables

Table 1: Mean and range of water table levels (relative to the local ground surface at the monitoring point) in the main hydrological units (Peats – P, Peaty Gley (PG) and Peaty Podzols (PP) of two of the transects (monitored at 15 minute intervals) over 12 month period 2012-13)

	Transect 1			Transect 2		
	P1	**PG2**	**PP1**	**P3**	**PG4**	**PP2**
Mean [cm]	-5.5	-31.7	-54.8	-30.5	-4.0	-51.9
StdDev [cm]	2.1	13.7	38.6	10.1	5.2	28.3
Max [cm]	-1.1	-6.9	3.7	1.0	10.6	-9.5
Min [cm]	-9.9	-73.0	-149.7	-63.2	-17.8	-152.4

Table 2. Mean, range and standard deviation of δ^2H (‰) in precipitation, stream flow, soil water (in peat (P1) and podzol (PP3) profiles) and groundwater (GW) in 2 wells (>2m deep) over two hydrological years 2011-13. Precipitation and streamflow samples were daily, soil water and groundwater were weekly.

	P	**Q**	**P1**	**P1**	**PP3**	**PP3**	**PP3**	**GW1**	**GW2**
Depth			10cm	30cm	10cm	30cm	50cm		
Mean	-53.5	-56.4	-54.3	-58.7	-56.7	-56.9	-56.3	-61.1	-60.7
Min	-147.3	-67.4	-61.4	-61.8	-82.9	-63.8	-63.4	-64.6	-63.3
Max	-8.3	-49.5	-42.9	-56.5	-42.2	-46.9	-48.9	-56.3	-57.6
Sd	20.4	2.8	4.59	1.1	11.1	4.4	3.8	1.7	1.4

List of Figures

1. **Figure 1** Bruntland Burn catchment showing (a) topography (with contours in m), (b) topographic wetness index, (c) geology and (d) soil cover (soil classes numbers indicate HOST class) in relation to ERT transects and monitoring locations (for groundwater levels) in the peat (P), peaty gley (PG) and peaty podzol (PP) soils.

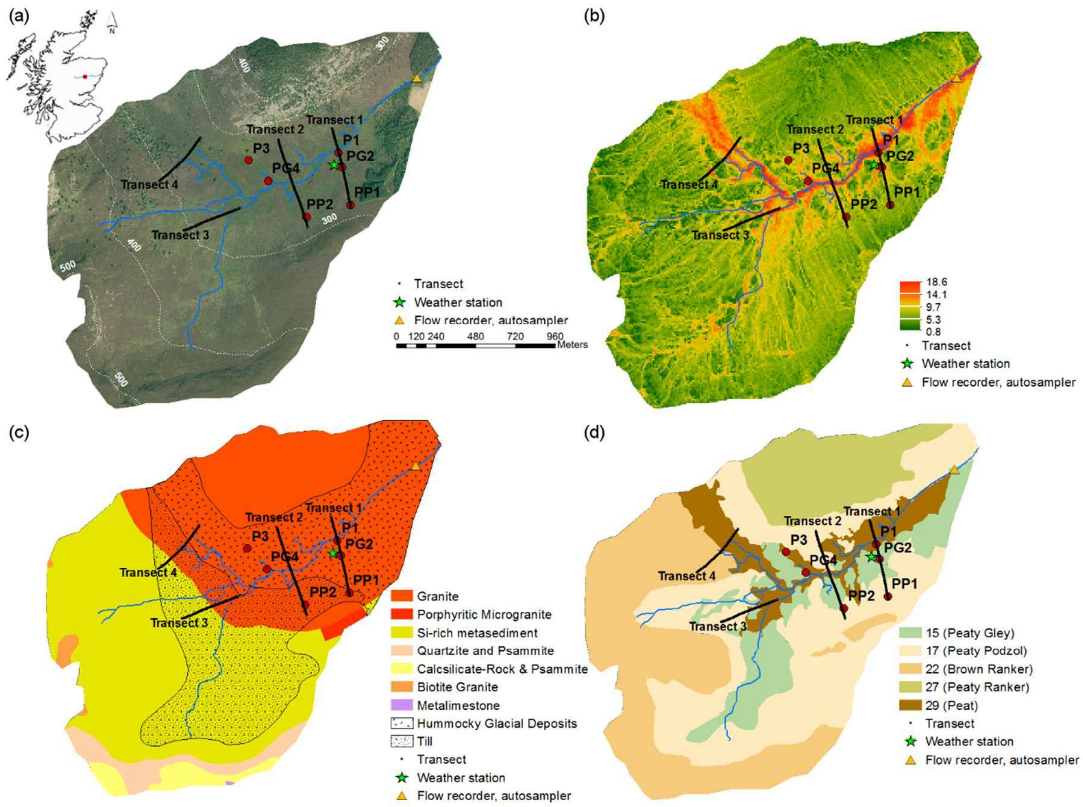

1. **Figure 2** Catchment rainfall-runoff response (top panel), precipitation isotopes (middle panel) and stream water isotopes (lower panel) 2012-2013.

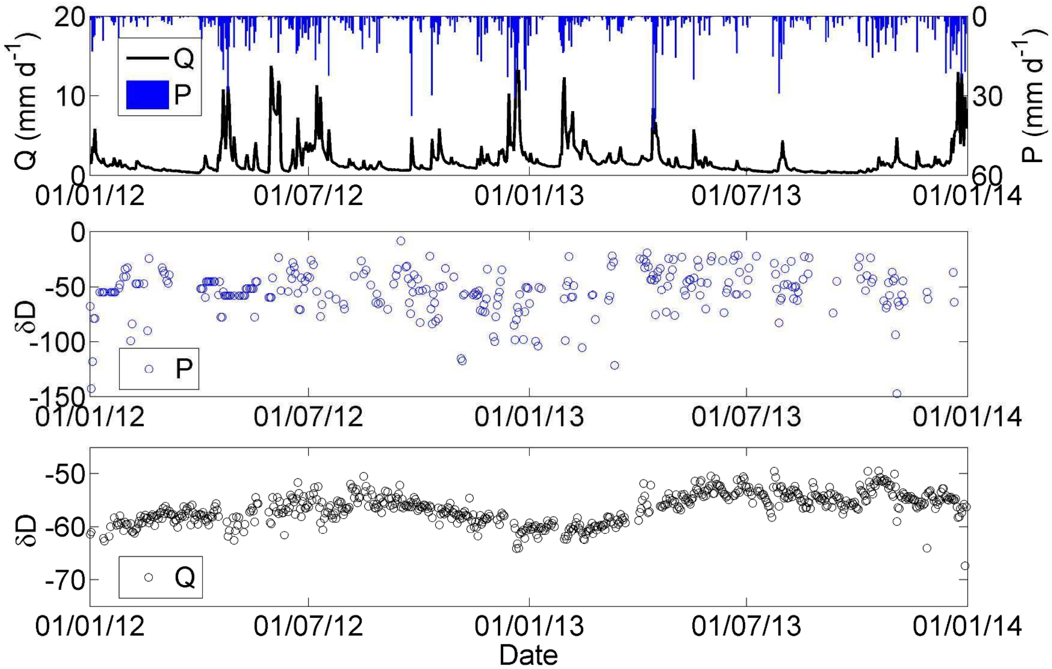

1. **Figure 3** Electrical resistivity (Ohm m) of the 4 transects: T1 (top panel) to T4 (bottom panel)

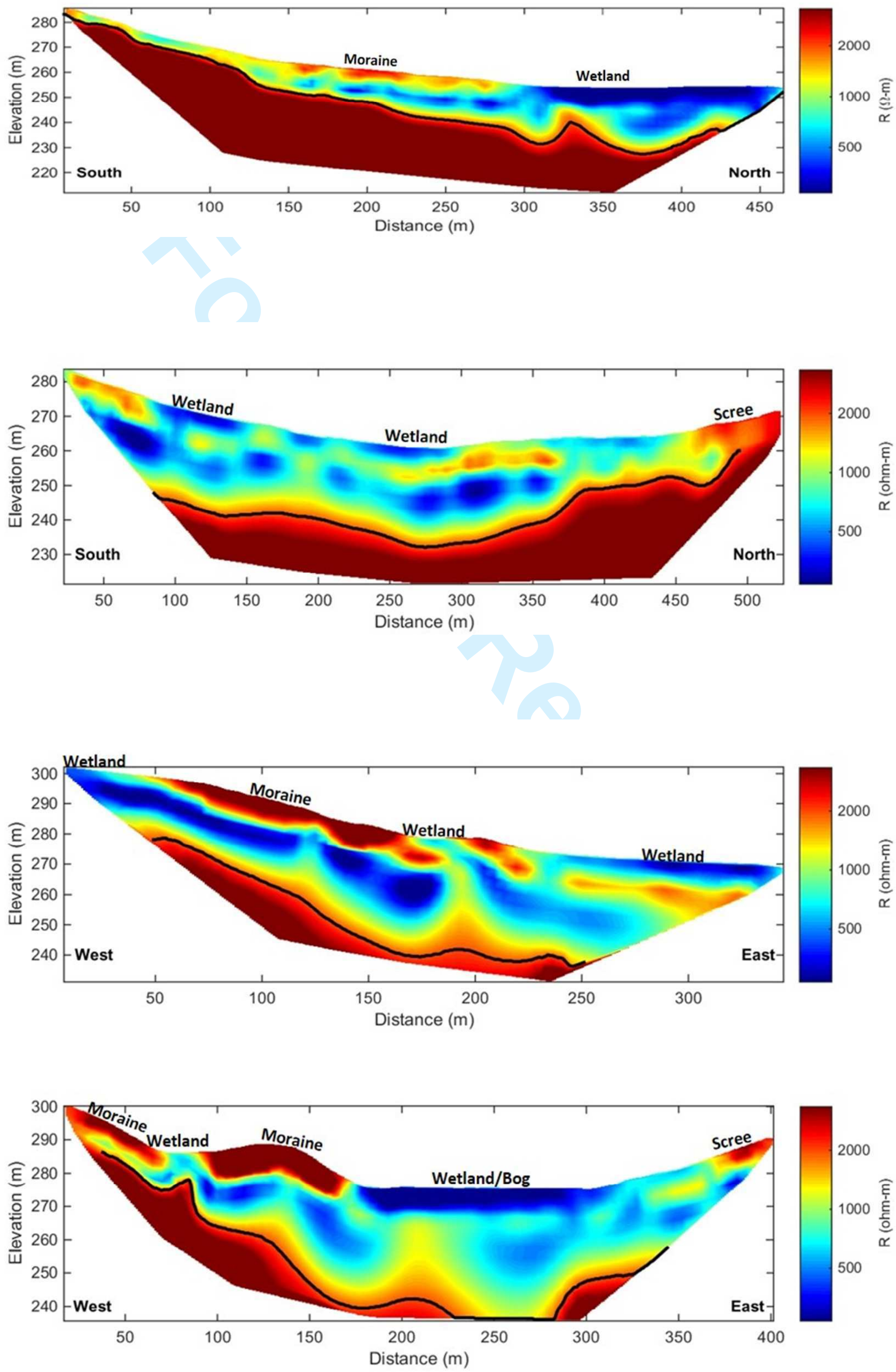

1. **Figure 4** Water content fraction along each transect: T1 (top panel) to T4 (bottom panel)

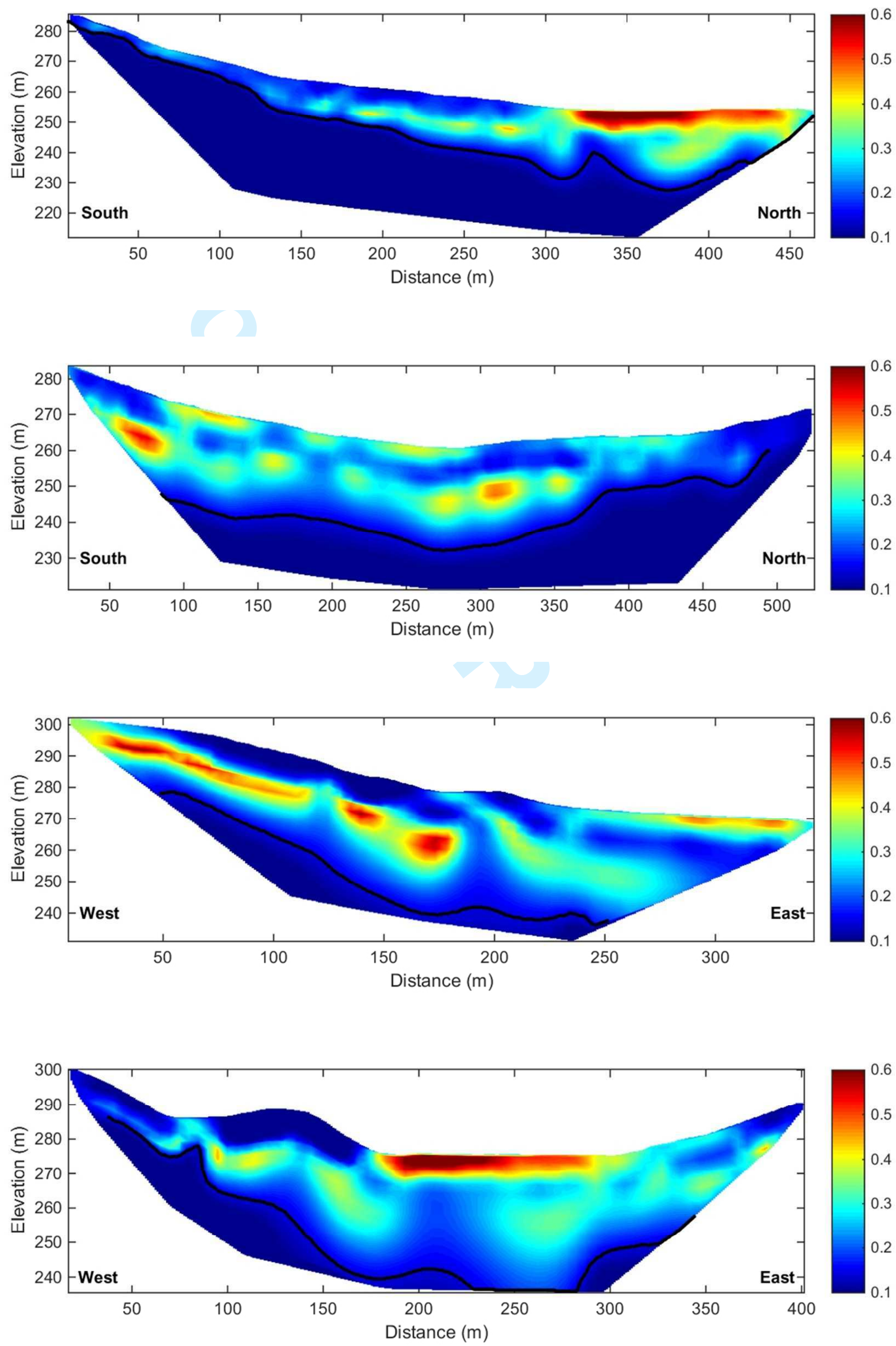

1. **Figure 5** Point water storage estimates (m) along each transect line

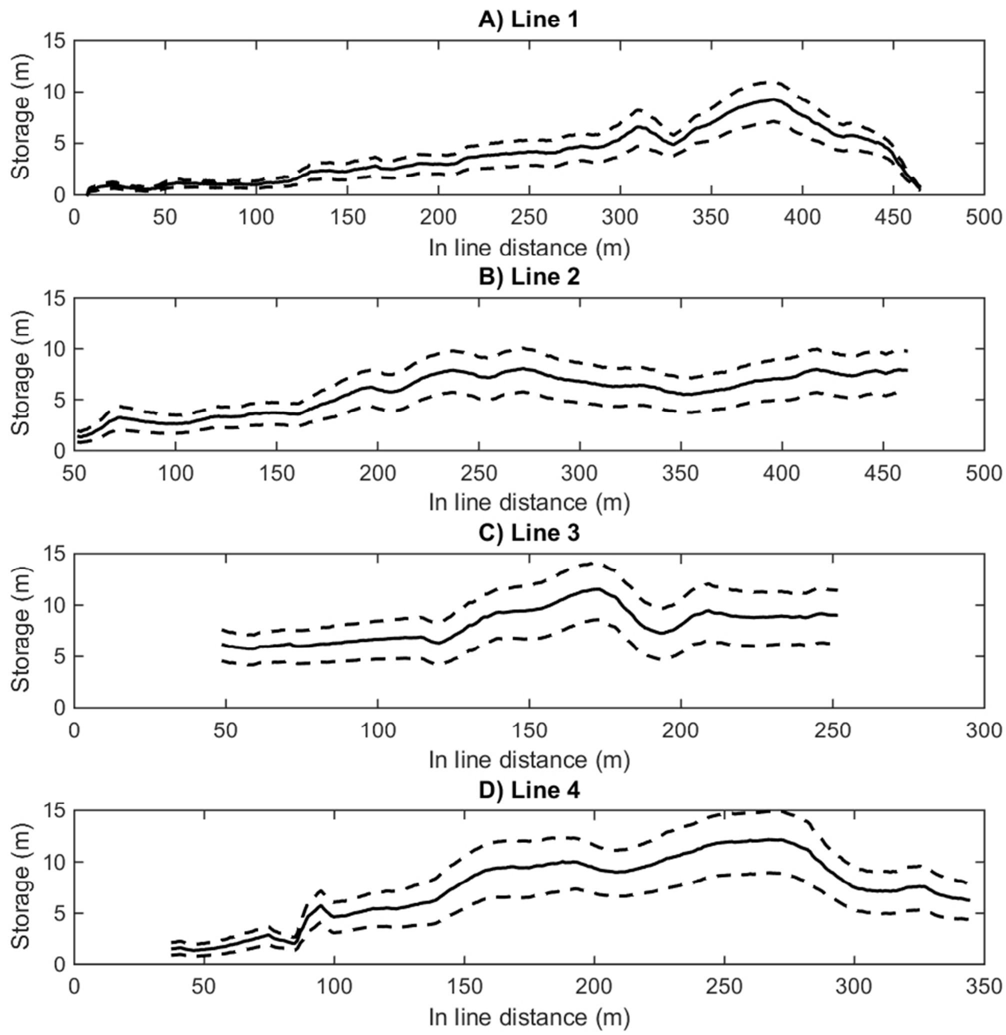

1. **Figure 6** Estimated spatial distribution of water storage at the catchment scale